DSTATCOM CONTROL TECHNIQUES: AN OVERVIEW

Abstract

This paper presents an overview of different control theories and control techniques associated with DSTATCOM; simulation results are presented. Results show the improvement in the power quality, at different stages with the connection of DSTATCOM.

To carry out the simulation, a small microgrid consisting of DG system, PV panel with constant and variable loads are considered. Considered microgrid is connected to the utility grid through PCC (point of common coupling), simulation is carried out when microgrid is connected to utility grid which acts as grid connected mode and as well as when microgrid is disconnected from utility grid, which acts as islanded mode. In both the modes of operation, power quality is observed at the load side.

Power quality in any AC grid is defined by three variables, load voltage magnitude, frequency at load and THD of load current.

It was observed through the simulation, Power quality at load side gets effected when working in islanded mode due to the variation in load, this leads to transients. These transients can be easily mitigated using properly designed DSTATCOM. The control signals required for DSTATCOM can be generated using different control techniques. Compression of different control techniques such as Instantaneous reactive power theory (IRP) with conventional PI controller, Synchronous reference frame (SRF), Hysteresis current controller and Model predictive controller (MPC) is presented. Simulation is carried out using MATLAB in Simulink environment.

Keywords: DSTATCOM; DG (Diesel Generator); IRP; MPC; Microgrid; PV System; SRF; THD.

Authors

Divya B V
School of EEE
REVA University
divya.bv@reva.edu.in

Dr. Archana N V
Department of EEE
NIE, Mysore
archananv@nie.ac.in

I. INTRODUCTION

With the increase in power demand and to reduce the consumption of fossil fuels for energy generation, we are moving towards renewable energy. To integrate renewables to the grid has lot of challenges associated with it. Where DG (Distributed generation) is a solution, distributed generation can be accomplished through Microgrids. These Microgrids can fulfil the needs of local remote areas and as well as can be connected to the utility grid, where excess power can be supplied to the grid. Whenever there is changeover from grid connected mode to islanded mode or vice versa and change in load, the microgrid goes through a transient, which can affect the power quality at the load side. If it is operating in grid connected mode, this can also lead to cascading effect.

Power quality issues and its mitigation has been of much attention these days, as it can affect the power consumers. These challenges can be addressed by properly compensating active and reactive power at the distribution side. As we concentrate on distributed side compensation, DSTATCOM can be the better option. DSTATCOM can provide reactive power compensation, can control voltage, and used to damp the oscillations [1] at low voltage side. It can enhance the power quality at distribution side. DTATCOM is a FACTS device, connected in parallel with the system and used solve all power quality problems at the distribution side. It generates or absorbs reactive power at PCC, to make sure that power quality is maintained, also it has a better dynamic response [2].

DSATCOM installed in any power system consists of 3 main parts: Voltage source converter (VSC); Coupling reactors; Controller.

DSTATCOM works on the principle where generation of AC power is controlled by Voltage source inverter (VSI), connected to energy storage device (Capacitor). Due to the voltage difference between the power system and DSTATCOM reactance, power transfer is caused. Switching signals to the VSI is provided through the feedback controller after measuring required voltage and current. Control of AC voltage is achieved through the firing angle control of semiconductor devices used in VSI. Hence controller plays a very important role. Fig1 represents the block diagram of a VSI based DSTATCOM.

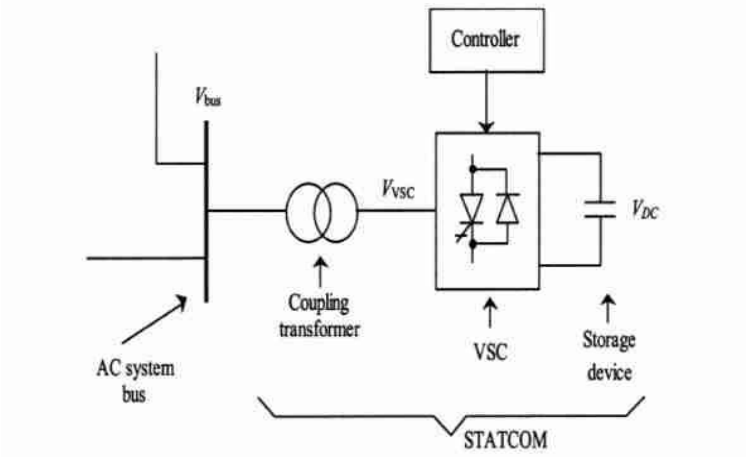

Figure 1: Block diagram representation of VSI based DSTATCOM.

Control algorithm used in the generation of control signals decides the performance of the DSTATCOM [3-16]. Hence in this paper an effort has been made to analyse different controllers used for DSTATCOM in a microgrid through simulation and results are presented at different operating conditions.

II. TOPOLOGIES

DSTATCOM can be operated with different topologies [17]. These topologies are used for multiple applications, for which DSTATCOM is designed.

Different topologies are: Three phase four wire system and three phase three wire system. To improve the power quality at distribution side three phase three wire topology,show better performance, as it consists of lesser switching devices. Figure 2. Below shows the structure of three phase three wire topology of DSTATCOM.

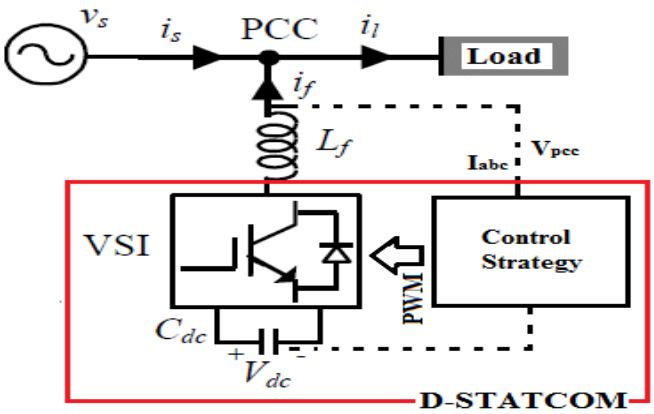

Figure 2: Structure of 3 phase 3 wire DSTATCOM

III. DESIGN OF DSATCOM

Figure 3 below shows the considered microgrid for simulation, consisting of constant load, variable load. For generation DG and PV array.

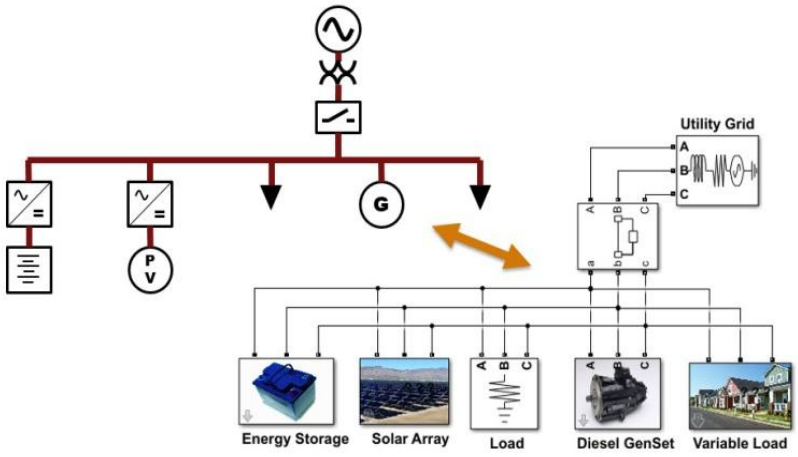

Figure 3: Microgrid

Here the utility grid with swing bus is operating at 13.8kV, transformer is 13.8kV/5kV. Voltage at PCC is considered as 5kV.

Constant load is 500kW and variable load consisting of both active and reactive load which can be varied.

Generating units DG can generate up to 1MW at 50 Hz, 5kV.

PV array is designed for 500kW at 5kV, connected through an inverter, to generate 3 phase power at 50 Hz. It is connected to grid using MPPT algorithm to the inverter control. DSTATCOM works on the principle of reactive power flow, depending on the voltage gradient. Considering two voltages V1 and V2 connected through the impedance Z, given by:

$$Z = Ra + jX \quad (1)$$

In the Fig 4 shown below Q represents reactive power flow, angle δ represents the angle between V1 and V2. If δ=0, the reactive power flow is given by:

$$Q = \left(\frac{V2}{X}\right)[V1 - V2] \quad (2)$$

Active power flow will become zero:

$$P = \frac{V1V2sin\delta}{X} \quad (3)$$

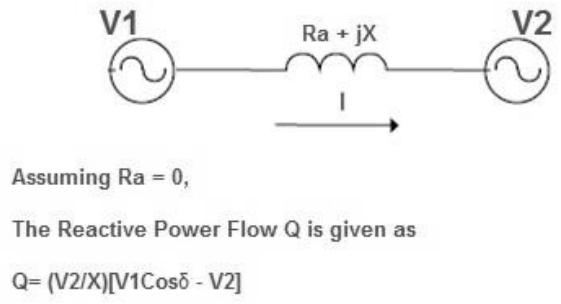

Figure 4: Working Principle of DSTATCOM

Following are the DSTATCOM components:

- Voltage source converter (VSC).
- DC source Capacitor.
- Inductive reactance.
- Harmonic filter.

To improve the power quality, load current expected at the load should be sinusoidal in nature.
Line current is described by the equation:

$$i_s = i_f + i_l \quad (4)$$

Where i_s - Represents the instantaneous value of line current.
i_f – Represents instantaneous value of compensating current.
i_l – Represents instantaneous value of load current.

Here VSC controlling is done by Pulse width modulation (PWM) technique. For designing the controller, design of DSTATCOM is important.
From the Fig 5 Shown, Instantaneous power at the load is represented by:

$$P_l(t) = P_f(t) + P_r(t) + P_h(t) \quad (5)$$

Where f- Represents fundamental component
r- Represents reactive power component.
h- Represents harmonic component.

$P_s = P_f$ ->Real power is supplied by the source
Q_s=0->Reactive power supplied by the source
$P_l = P_f + P_h$ ->Real power drawn by the load
$Q_l = Q_f + Q_h$->Reactive power drawn by the load

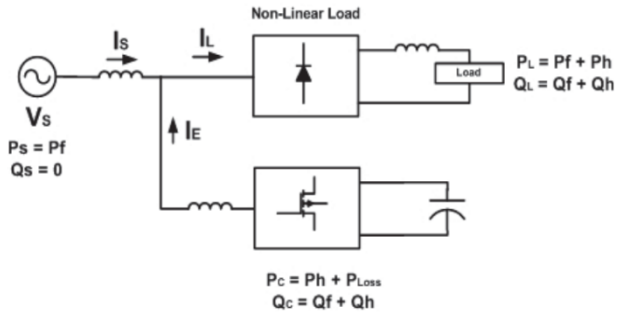

Figure 5: Compensation Technique Representation

Real power supplied by the compensator $P_c = P_h – P_{loss}$
Reactive power supplied by the compensator $Q_c = Q_f + Q_h$
P_{loss} – Loss component of the capacitor.

From the Figure 5.

$$I_s(t) = I_l(t) + I_e(t) \quad (6)$$

We know that:

$$V_s(t) = V_m \sin(\omega t) \quad (7)$$

Load current will have a fundamental component as well as harmonic components, represented by:

$$I_L(t) = \sum_{n=1}^{\infty} I_n \sin(n\omega t + \varphi_n) \quad (8)$$

$$I_L(t) = I_1 \sin(\omega t + \varphi_1) + \sum_{n=2}^{\infty} I_n \sin(n\omega t + \varphi_n) \quad (9)$$

Instantaneous power at load can be expressed as:

$$P_l(t) = V_s(t) I_l(t) \quad (10)$$

$$P_l(t) = V_m \sin(\omega t) I_1 \sin(\omega t + \varphi_1) + V_m \sin(\omega t) \sum_{n=2}^{\infty} I_n \sin(n\omega t + \varphi_n) \quad (11)$$

$$P_l(t) = V_m I_1 sin^2 \omega t \, cos\varphi_1 + V_m I_1 sin\omega t \, cos\omega t \, sin\varphi_1 + V_m sin\omega t \sum_{n=2}^{\infty} I_n \sin(n\omega t + \varphi_n) \quad (12)$$

We know that:

$$P_l(t) = P_f(t) + P_r(t) + P_h(t) \quad (13)$$

Where:

$$P_l(t) = P_f(t) + P_c(t) \quad (14)$$

At ideal conditions only the real fundamental component should be supplied by the source and rest all should be supplied by compensators. Hence

$$P_c(t) = P_r(t) + P_h(t) \quad (15)$$

Where $P_r(t)$ can be written as:

$$P_r(t) = V_s(t) I_s(t) \quad (16)$$

i.e.

$$I_s(t) = \frac{P_r(t)}{V_s(t)} = I_{sm} \sin(\omega t) \quad (17)$$

Hence the total maximum current supplied by the source:

$$I_{max} = I_{sm} + I_{sl} \quad (18)$$

Instantaneous current delivered from the source is represented as:

$$I_s(t) = I_{max} \sin(\omega t) \quad (19)$$

Desired source current is expected to be sinusoidal in nature irrespective of the load, hence the source current after compensation is given by:

$$I_{sa}^{*}(t) = I_{max}\ \sin(\omega t) \tag{20}$$

$$I_{sb}^{*} = I_{max}\ \sin\left(\omega t - \frac{2\pi}{3}\right) \tag{21}$$

$$I_{sc}^{*} = I_{max}\ \sin\left(\omega t - \frac{4\pi}{3}\right) \tag{22}$$

These are the desired source currents; hence the above currents are taken as reference currents for the 3 phases.

For the design of DSTATCOM:

i) DC Voltage:

$$V_{dc} = \frac{2\sqrt{2}V_{LL}}{\sqrt{3}m} \tag{23}$$

Where $V_{LL}$is 5kV and m is chosen as 1.
Substituting this in equation (23), V_{dc} is calculated as 9000V or 9kV.

ii) Design of DC bus capacitor:

$$\left(\frac{1}{2}\right) C_{dc}(V_{dc}^{2} - V_{dc1}^{2}) = K_1 3aIt \tag{24}$$

Where:
V_{dc1} -> Minimum DC bus voltage 5kV
a-> Overloading factor chosen to be 1.2
I -> Phase current is 100Amps
t -> Time by which the DC bus voltage recovers, 30msec
K_1 -> 0.1(considering 10% energy variation)

Using the above equation (24)C_{dc} is calculated as 500µF.

iii) Selection of AC inductor:
AC inductance

$$L_r = \frac{\sqrt{3}mV_{dc}}{12af_sI_{cr,pp}} \tag{25}$$

From the above equation:
m -> Modulation index =1
$I_{cr,pp}$ -> Current ripple 15%
F_s -> Switching frequency = 1.8kHz

V_{dc} = 9000V
a =1.2

Using the above equation (25) $L_r$is calculated as 720mH.

iv) For ripple filter:
C= 5µF
R=5Ω

IV. CONTROL TECHNIQUES

As the performance of the DSTATCOM depends on control techniques used to generate control signals to the switches. Some of the control techniques that will be considered in this paper for the analysis are IRP, SRF, Hysteresis current controller and MPC.

1. **Instantaneous Reactive Power Theory (IRPT) with Conventional PI Controller:** IRP theory can be applied for both three phase three wire system and three phase four wire system. This theory was proposed by Akagi [18] is also known as p-q theory. In this technique three phase instantaneous load current and voltage are transformed to 2 phase in α-β frame, by Clark's transformation. In this frame instantaneous value of active and reactive powers are calculated.

   Using reverse clark's transformation the reference currents in α-β frame is transformed into abc frame. Figure 6: Shows the block diagram of IRP technique.

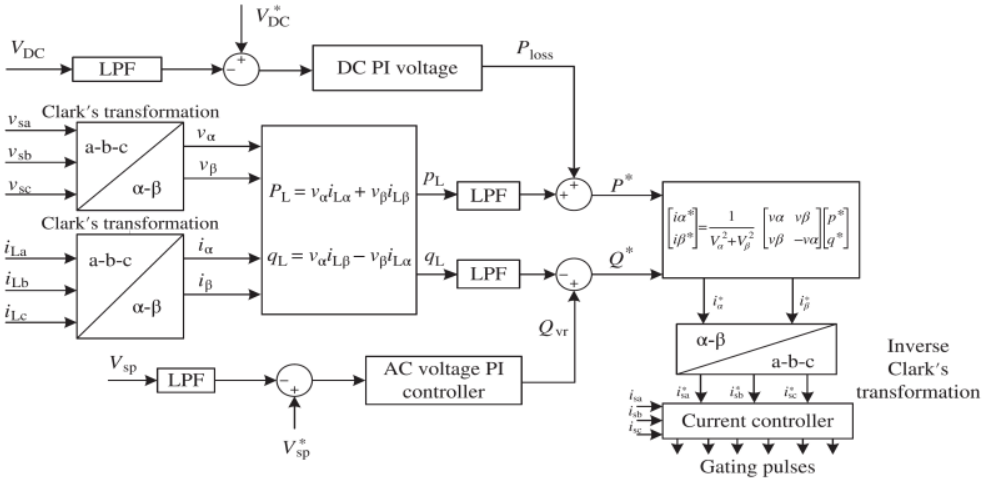

Figure 6: Block Diagram of IRP technique

$$\begin{bmatrix} v_\alpha \\ v_\beta \end{bmatrix} = \sqrt{\frac{2}{3}} \begin{bmatrix} 1 & -1/2 & -1/2 \\ 0 & \sqrt{3}/2 & -\sqrt{3}/2 \end{bmatrix} \begin{bmatrix} v_a \\ v_b \\ v_c \end{bmatrix} \quad (26)$$

$$\begin{bmatrix} i_\alpha \\ i_\beta \end{bmatrix} = \sqrt{\frac{2}{3}} \begin{bmatrix} 1 & -1/2 & -1/2 \\ 0 & \sqrt{3}/2 & -\sqrt{3}/2 \end{bmatrix} \begin{bmatrix} i_a \\ i_b \\ i_c \end{bmatrix} \tag{27}$$

Instantaneous values of active and reactive powers are given by:

$$\begin{bmatrix} p \\ q \end{bmatrix} = \begin{bmatrix} v_\alpha & v_\beta \\ -v_\beta & v_\alpha \end{bmatrix} \begin{bmatrix} i_\alpha \\ i_\beta \end{bmatrix} \tag{28}$$

The reference currents in α-β is given by:

$$\begin{bmatrix} i^*_{s\alpha} \\ i^*_{s\beta} \end{bmatrix} = \frac{1}{\Delta} \begin{bmatrix} v_\alpha & -v_\beta \\ v_\beta & v_\alpha \end{bmatrix} \begin{bmatrix} p \\ 0 \end{bmatrix} \tag{29}$$

Where $\Delta = v_\alpha^2 + v_\beta^2$. To calculate the reference currents in abc frame, using reverse clark's transformation:

$$\begin{bmatrix} i^*_{sa} \\ i^*_{sb} \\ i^*_{sc} \end{bmatrix} = \sqrt{\frac{2}{3}} \begin{bmatrix} 1/\sqrt{2} & 1 & 0 \\ 1/\sqrt{2} & -1/2 & \sqrt{3}/2 \\ 1/\sqrt{2} & -1/2 & -\sqrt{3}/2 \end{bmatrix} \begin{bmatrix} i^*_0 \\ i^*_{s\alpha} \\ i^*_{s\beta} \end{bmatrix} \tag{30}$$

The 3phase reference current is generated using the above equation (30), using conventional PI controller to generate the error signals. Switching signals to the VSI are generated using PWM technique.

Fig 7 shows the simulation carried out using IRT:

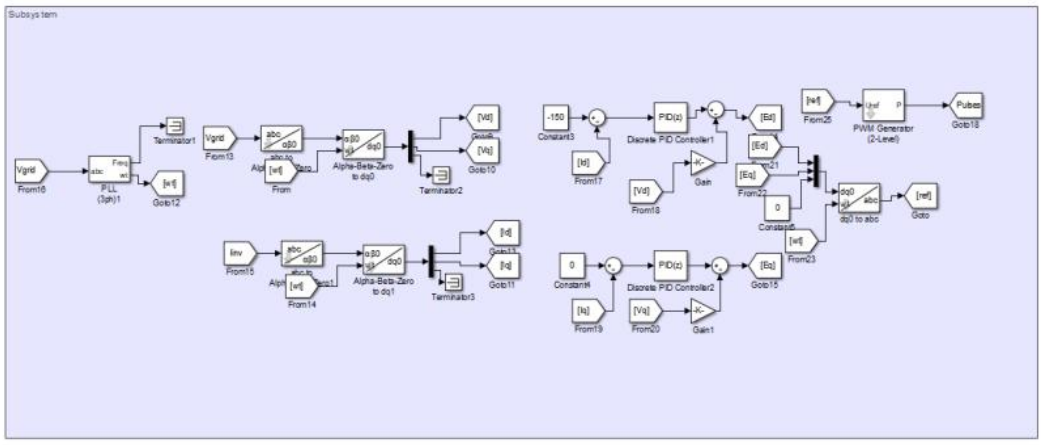

Figure 7 Simulation Model of IRT using conventional PI controller

2. **Synchronous Reference Frame (SRF) with Conventional PI Controller:** Synchronous reference frame is called as dq-control, grid voltage and current are converted into rotating frame, which rotates synchronously with grid voltage vector using park

transformation. It is the popularly used Phase locked loop (PLL) method, which will supply the average values of frequency, voltage magnitude and phase angle. PLL is used to generate sine and cosine templets of voltage signal. Fig 8 shows the block diagram representation of SRF controller.

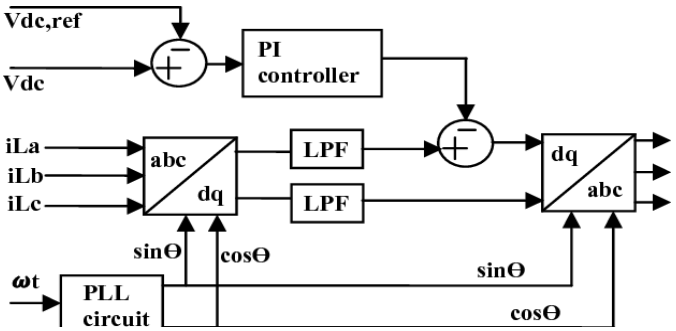

Figure 8: Block diagram representation of SRF controller

SRF theory is based on transforming 3 phase current into dq frame, which is synchronously rotating, if θ is the transformation angle, current transformation from αβ to dq frame is given by:

$$\begin{bmatrix} i_d \\ i_q \end{bmatrix} = \begin{bmatrix} cos\theta & sin\theta \\ -sin\theta & cos\theta \end{bmatrix} \begin{bmatrix} i_\alpha \\ i_\beta \end{bmatrix} \tag{31}$$

DC component extracted are changed back to αβ frame using:

$$\begin{bmatrix} i_{\alpha dc} \\ i_{\beta dc} \end{bmatrix} = \begin{bmatrix} cos\theta & sin\theta \\ -sin\theta & cos\theta \end{bmatrix} \begin{bmatrix} i_{ddc} \\ i_{qdc} \end{bmatrix} \tag{32}$$

The gate pulses to the switches of VSC is generated using PWM technique, which is used to mitigate reactive power and harmonic current. Fig 9 shows the SRF controller implemented in Matlab/Simulink.

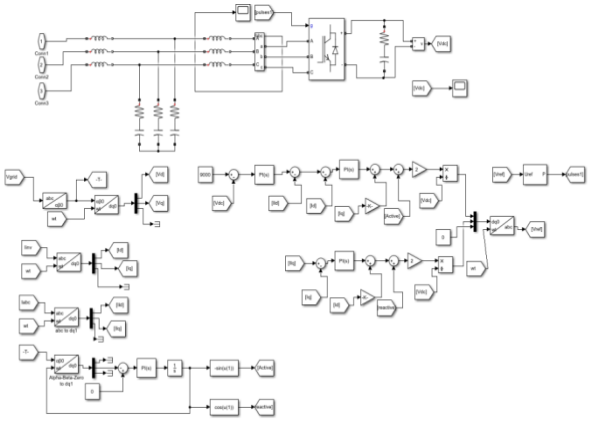

Figure 9: SRF Controller Implementation in Matlab/Simulink

3. **IRP using Hysteresis Current Controller:** Hysteresis current control method is used with three phase VSC PWM inverter with current control, it allows Phase locked loop (PLL) control for modulating the frequency of inverter switches, thus allowing minimum interface between the switches. Fig 10 shows the block diagram representation of the Hysteresis current controller.

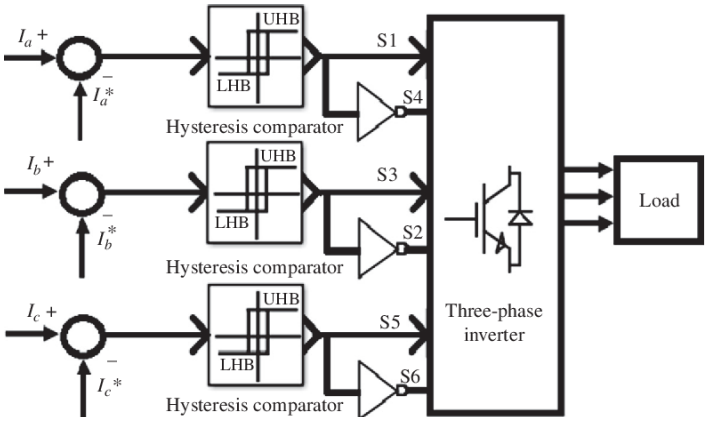

Figure 10: Block diagram of Hysteresis current controller

In hysteresis controller, the control circuit limits the signals on either side, so that the desired output is obtained. The reference sine wave with desired magnitude and frequency is generated by the control circuit and this is compared with the actual signal. Based on this the inverter switches are operated, so that the signals generated are within the limits. Fig 11 shows the basic principle of a hysteresis controller. Here the reference current and the fault current are given to the summer, the combination of these currents is given to the relay circuit, to limit the fault current, accordingly the gating pulses are generated to the switches, which operates the three-phase inverter.

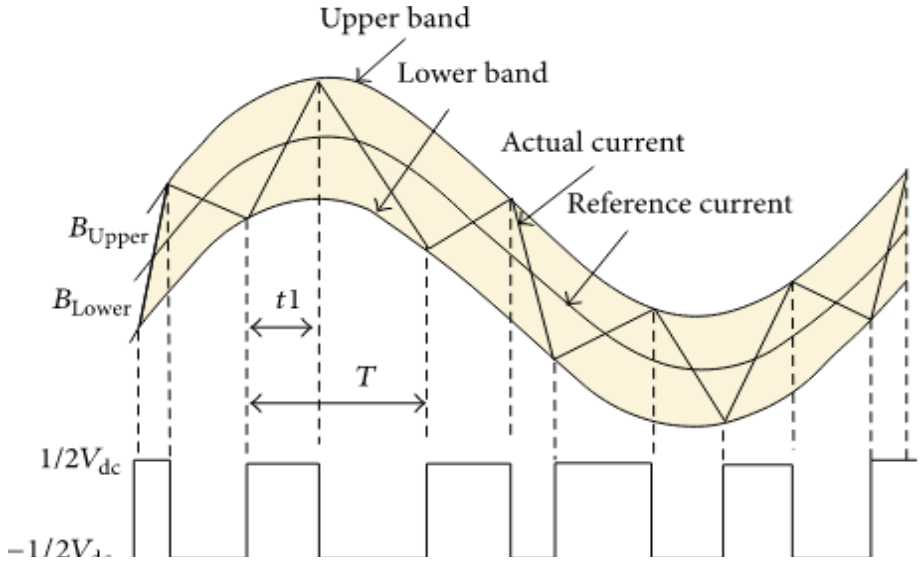

Figure 11: Basic Principle of Hysteresis Controller

Figure 12 shows the MATLAB/Simulink implementation of Hysteresis current controller.

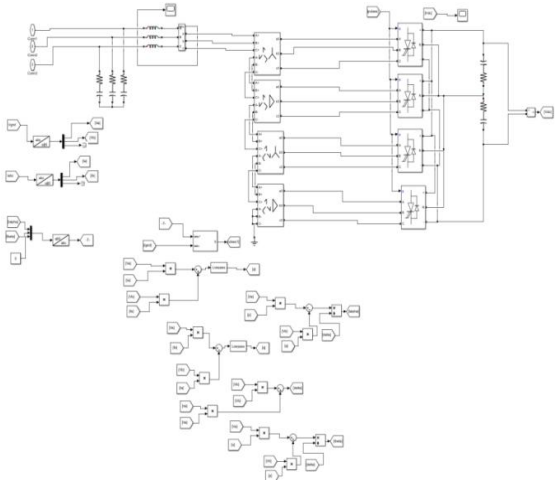

Figure 12: Implementation of Hysteresis controller in Matlab/Simulink

4. **IPR Using Model Predictive controller:** It is a type of feedback control, based on the predictive model of any process Model Predictive control algorithm is designed. Here model of the plant is used to predict the future output of the considered plant.

   This is a optimisation algorithm for which cost function needs to be designed, as desired output needed is sinusoidal output voltages, without any disturbance. To achieve this the error between the output voltage predicted and the reference voltage should be minimized. Equation below represents the cost function represented by g_N in equation (33), which is expressed in orthogonal coordinate format, and this defines the desired behaviour of the system.

$$g_N = (v_{c\alpha}^* - v_{c\alpha}(k+N))^2 + (v_{c\beta}^* - v_{c\beta}(k+N))^2 \quad (33)$$

   $V^*_{c\alpha}$ & $V^*_{c\beta}$ represents real and imaginary parts of voltage output reference vector of V_c. Where $V_{c\alpha}$ & $V_{c\beta}$ represents real and imaginary parts of predicted output voltage $V_c(K+N)$.
   Using this PWM signals are generated for the inverter connected to DTATCOM Figure 13: shows the implementation of MPC in Matlab/Simulink.

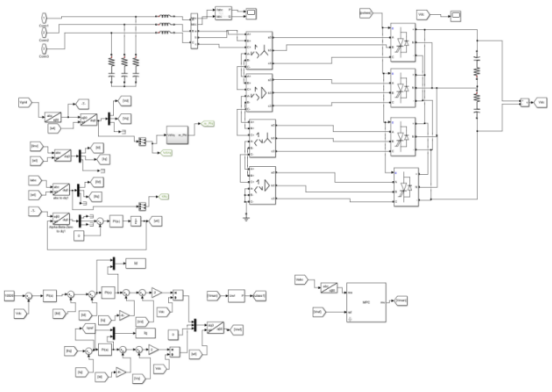

Figure 13: Implementation of MPC in Matlab/simulink

V. RESULTS AND DISCUSSION

Wave forms show the results obtained from different types of control techniques. Simulation is carried out in Matlab/Simulink for the considered microgrid for 1sec and the results are presented .Results are obtained for both grid connected mode as well as islanded mode. Fig 12 shows the output of the microgrid, without DSTATCOM.

Here simulation is carried out for 1se, where at 0.5sec the microgrid gets disconnected from the utility grid and at 0.6, 0.7 sec there is change in the load. During the load change the transients can be observed in the load voltage. Power factor is also calculated at the load voltage, which shows a very high dip in the pf during load changeover. Fig 14 shows the power factor at the load side. These transients can be eliminated by connecting DSTATCOM parallel to the microgrid.

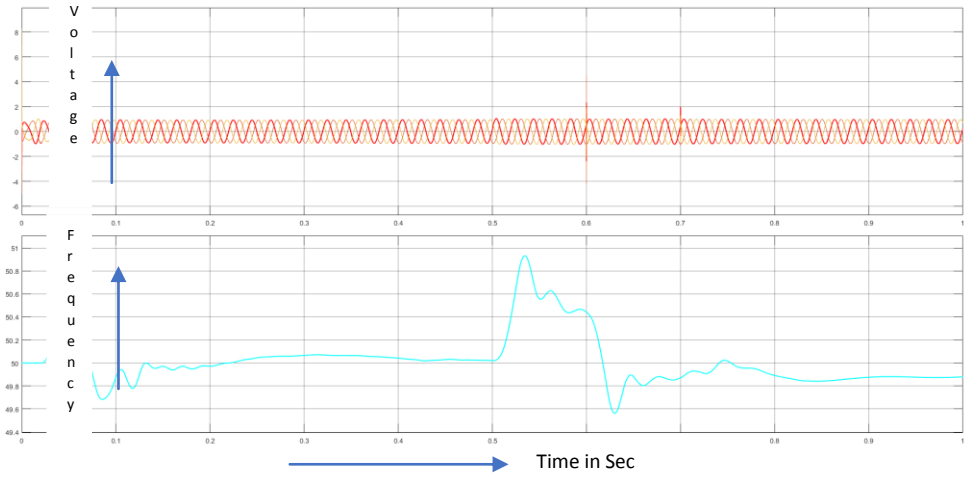

Figure 14: Output of Microgrid without DTSTCOM

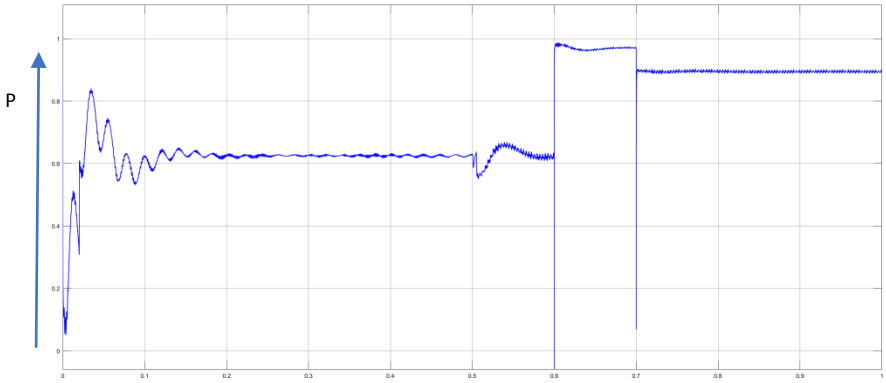

Figure 15: Load power factor without DSTATCOM

Results are presented with DSTATCOM connected to the microgrid in parallel. Fig 16 shows the Simulink block diagram of the considered microgrid, with DSTATCOM connected in parallel, with different types of controllers.

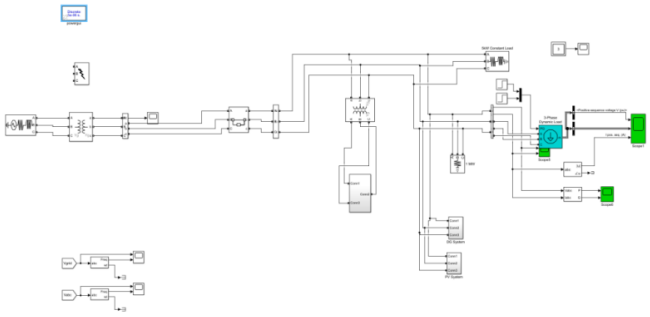

Figure 16: Block diagram of DSTATCOM connected in parallel.

1. **IRP Theory with Conventional PI Controller:** Fig 17 shows the output of the IRP theory with conventional PI controller, where it is observed from that during load change, there are voltage transients, but frequency is observed to be almost constant. Fig 18 shows THD analysis carried out for output current at different intervals for grid changeover and load change.

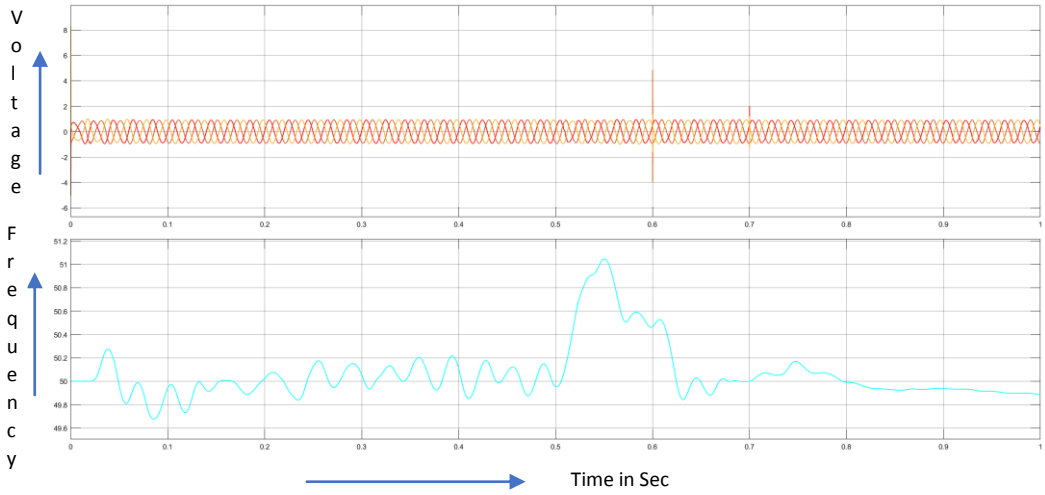

Figure 17: Output Voltage and Frequency of IRP theory with PI controller.

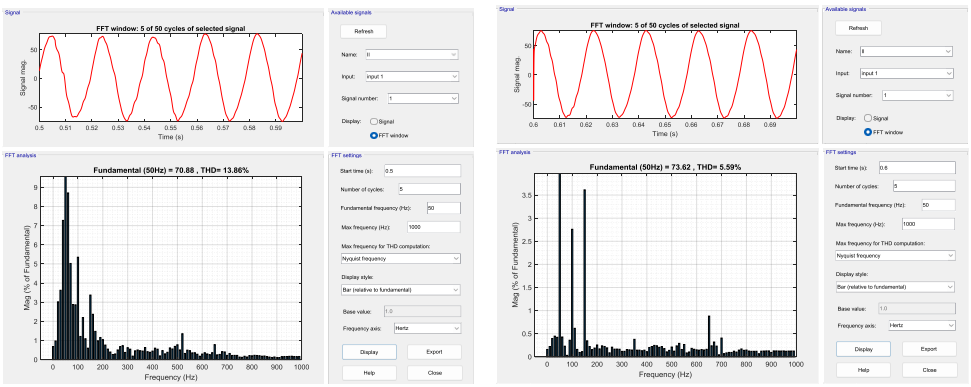

Figure18: THD Window of IRP Theory with PI Controller.

From the above results it is observed that the THD is 13.86% and 5.6 % not within the acceptable limits and even the voltage magnitude is observed to have transients during load change.

2. **SRF with Conventional PI Controller:** Fig 19 shows the output of SRF with conventional PI controller, here the voltage transients can be observed during load change over and observed the dip in frequency. Fig 20 show the THD window carried out for load current, at different intervals of grid change and load change over. Here the THD is observed to be 11.33%, even though there is improvement in THD compared to IRPT method, this not acceptable for industrial loads. In this controller, its observed there is dip in load frequency also.

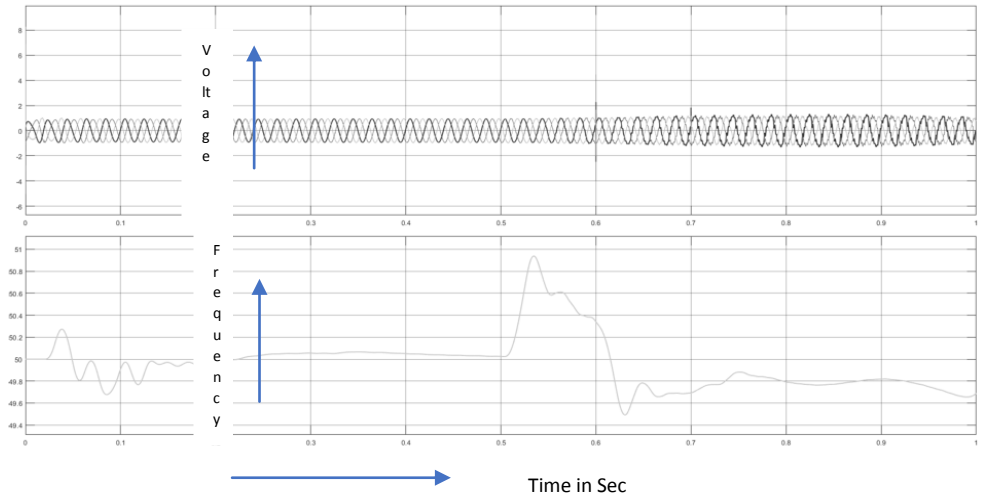

Figure 19: Output Voltage and Frequency of SRF with conventional PI controller.

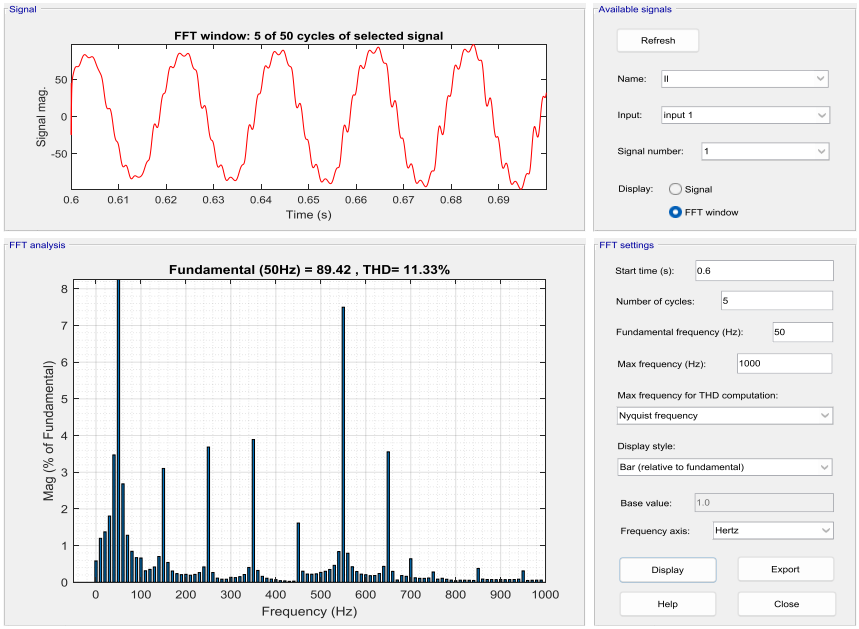

Figure 20: THD of SRF with conventional PI controller.

3. **Hysteresis Current Controller:** Fig 21 shows the simulation output of voltage and frequency of the microgrid using Hysteresis controller for the DSTATCOM.

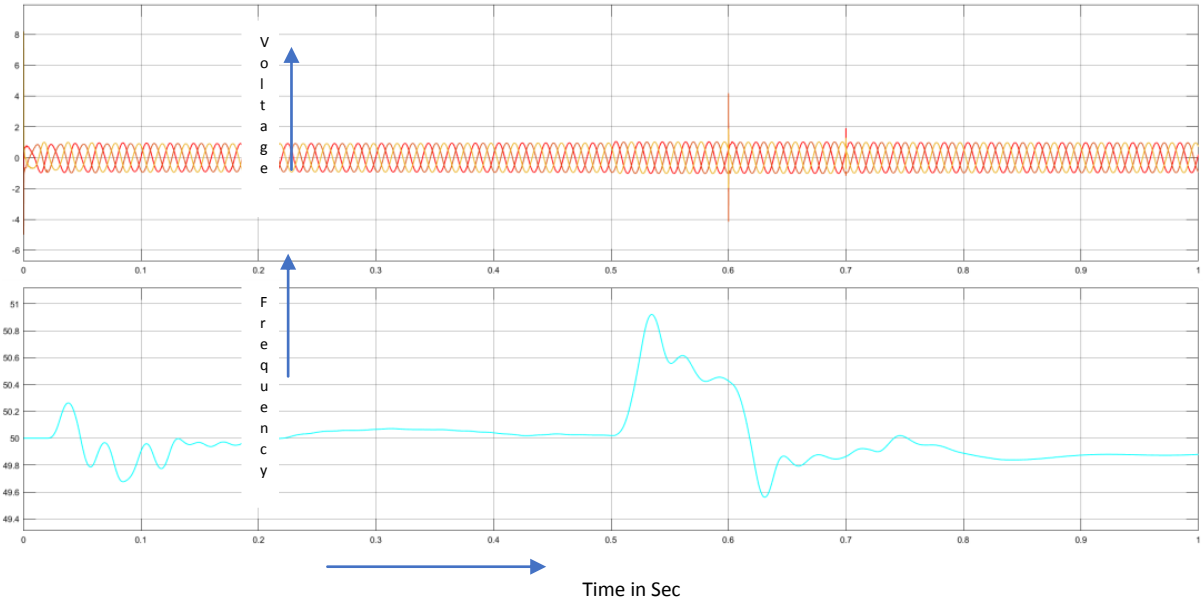

Figure 21: Output Voltage and Frequency of Hysteresis controller

In the above figure its observed that, even though frequency variation is small, voltage transients can be observed during the load change.

The THD window shows the improvement in the load current quality, but still voltage transients can be observed during load change 8.18% and 2.6%.

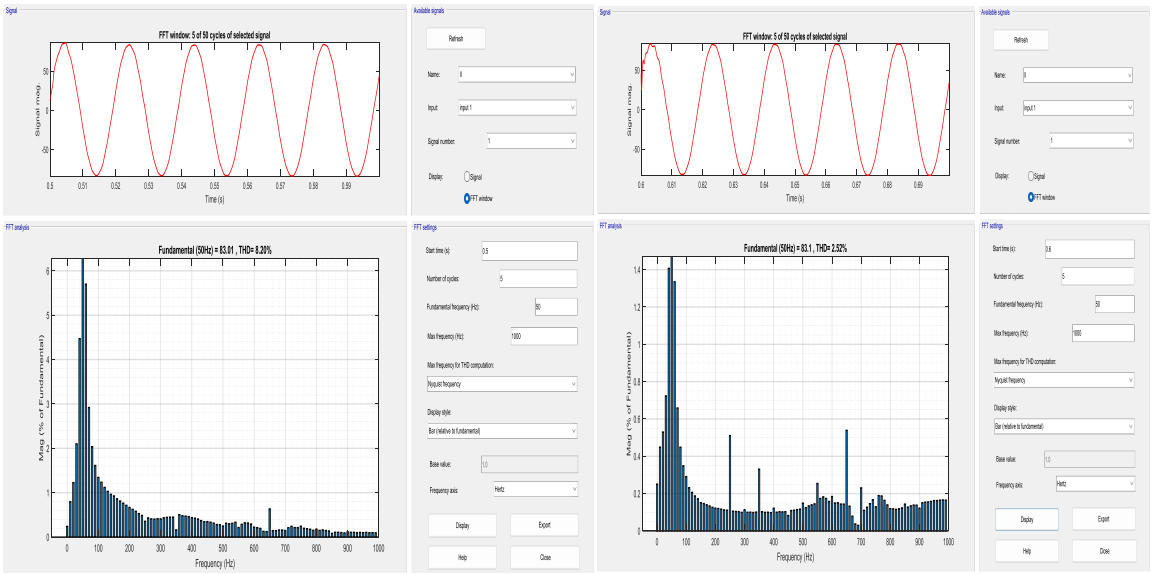

Figure 22: THD of Hysteresis controller

4. **MPC Controller:** Figure 23: Below shows the output Voltage and frequency of load voltage using MPC controller.

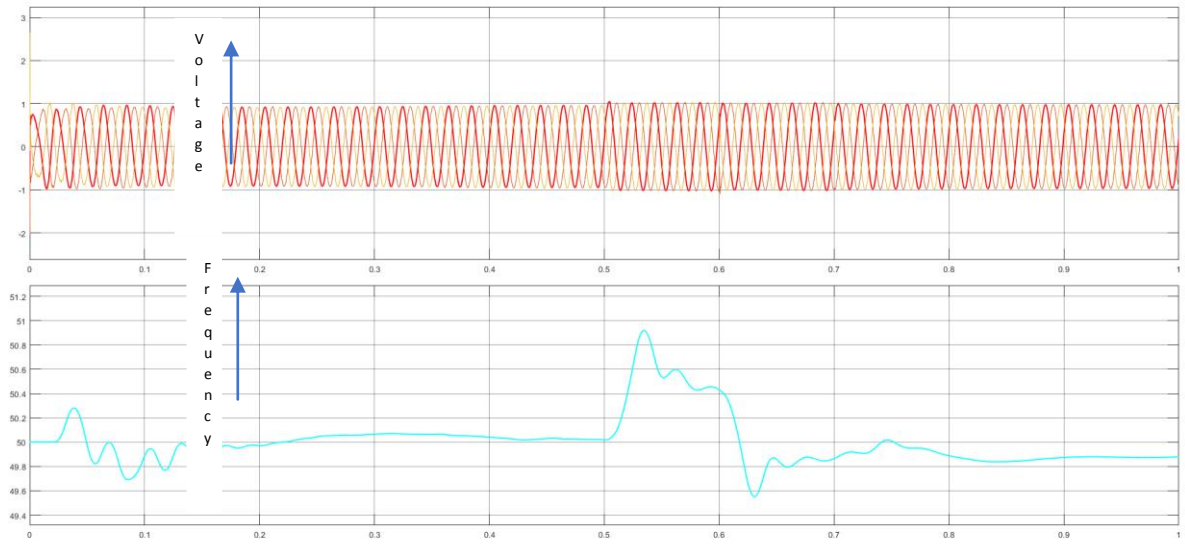

Figure 23: Output Voltage and Frequency of MPC controller

It's observed from the above figure, the voltage and frequency are in the limits. There are no voltage transients during the load change. THD analysis is carried out for the load current.

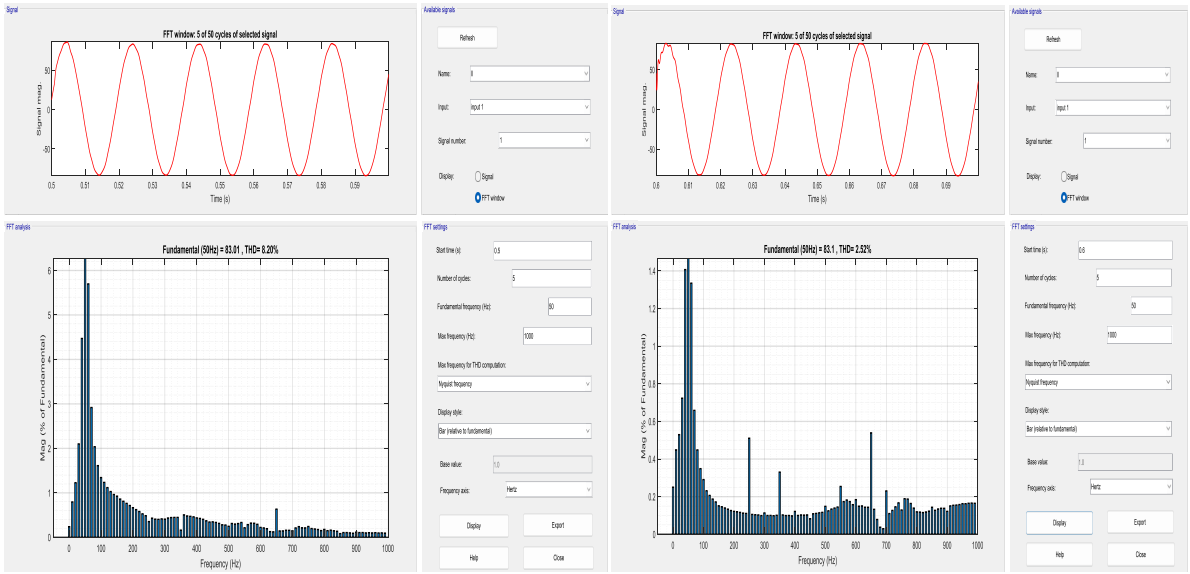

Figure 24: Output Voltage and Frequency of MPC controller

It's observed the THD is 8.2% and 2.52% during grid change and load change respectively. This shows the load current THD are improved and is within the industry acceptable limits.

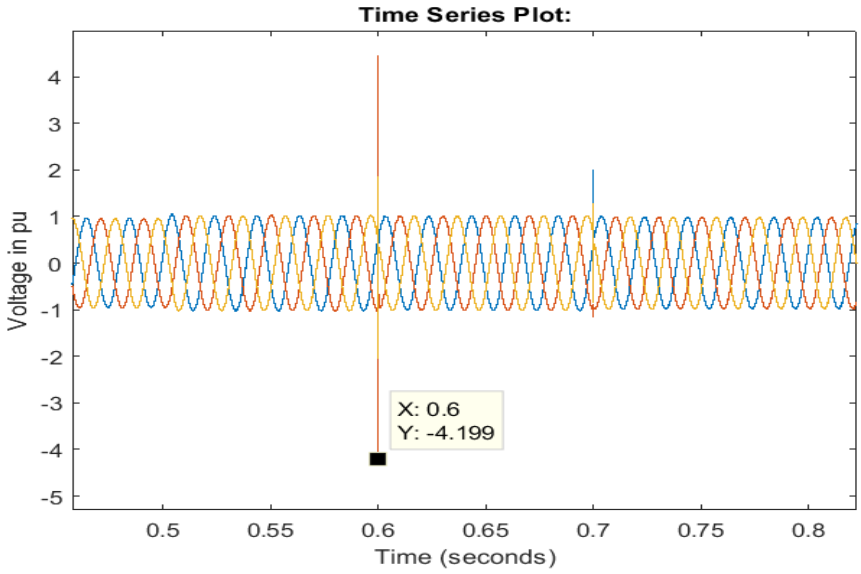

Figure 25: Output Voltage before compensation

Figure 25 shows the load voltage before compensation and fig 26 shows the load voltage after compensation in pu.

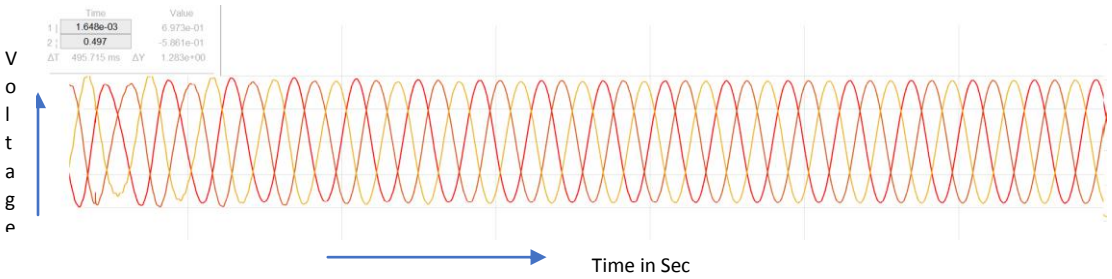

Figure 26: Output Voltage after compensation

Table 1 shows the comparison of different algorithms with their advantage and disadvantages, in reference to the simulation results obtained.

Table 1: Comparison of Different Control Algorithms.

Sl No.	Control Algorithm	Advantages	Disadvantages
1.	IRPT	Requires complex transformation	*Frequency can be controlled. here is no improvement in voltage Magnitude
2.	SRF	It is used for reducing harmonics	* Dip in frequency
3.	Hysteresis Controller	Improvement in Harmonics and frequency.	*Transient in load Voltage during load change over

4.	MPC	Implementation is easy, its observed it provides very good dynamic and steady state stability.	*For Using weighting factor, additional two constraints has to be added.

VI. CONCLUSION

DSTATCOM control techniques are reviewed for power quality enhancement, with the simulation results. The techniques reviewed are IRP, SRF, Hysteresis control and MPC, which is used to improve the power quality at the load, for a microgrid. Considering load Power factor, load Voltage magnitude, Load frequency and THD of the load current. From the Table 3, it can be observed that IRPT even though it requires complex calculations, frequency can be controlled, but voltage magnitude and THD during dynamics do not show much improvement. SRF controller, which shows improvement in harmonics, there is dip in frequency. Hysteresis controller shows improvement in harmonics and frequency, load voltage has transients during dynamics. The MPC controller show the better performance by improving the power quality in terms of voltage magnitude, frequency and as well as THD of load current. Also, it is observed with the inclusion of the DSTATCOM, there is improvement in load Power factor during Dynamics. Hence from the results, it can be concluded that compared to conventional PI controller, the heuristic controllers such as Hysteresis and MPC provides better performance during dynamics.

REFERENCES

[1] Divya B V, Dr. Archana N V, March 2020. Placement andcoordinated facts devices: An overview, IJSTR, Volume 9, pp.1520-1523.
[2] Divya, B.V., Archana, N.V., Latha, N. and Surendra, U., 2022, October. Small signal stability in a Microgrid using PSO based Battery storage system. In 2022 IEEE Industrial Electronics and Applications Conference (IEACon) (pp. 55-60). IEEE.
[3] Jyothi, K.R.S., Kumar, P.V. and JayaKumar, J., 2021. A Review of Different Configurations and Control Techniques for DSTATCOM in the Distribution system. In E3S Web of Conferences (Vol. 309). EDP Sciences.
[4] Varshney, G., 2013, April. Simulation and analysis of controllers of DSTATCOM for power quality improvement. In Conference on Advances in Communication and Control Systems (CAC2S 2013) (pp. 271-276). Atlantis Press.
[5] Shi, J., Noshadi, A., Kalam, A. and Shi, P., 2015, September. Fuzzy logic control of DSTATCOM for improving power quality and dynamic performance. In 2015 Australasian universities power engineering conference (AUPEC) (pp. 1-6). IEEE.
[6] Badoni, M., Singh, A., Semwal, S. and Tatte, Y., 2021. Control of DSTATCOM using nonparametric variable step-size NLMS: An experimental study. Electric Power Systems Research, 199, p.107411.
[7] Chawda, G.S. and Shaik, A.G., 2019, December. Adaptive reactive power control of dstatcom in weak ac grid with high wind energy penetration. In 2019 IEEE 16th India Council International Conference (INDICON) (pp. 1-4). IEEE.
[8] Kumar, A.P., Kumar, G.S., Sreenivasarao, D. and Myneni, H., 2019. Model predictive current control of DSTATCOM with simplified weighting factor selection using VIKOR method for power quality improvement. IET Generation, Transmission & Distribution, 13(16), pp.3649-3660.
[9] Singh, B., Dube, S.K. and Arya, S.R., 2015. An improved control algorithm of DSTATCOM for power quality improvement. International Journal of Electrical Power & Energy Systems, 64, pp.493-504.
[10] Mishra, S., Sreejith, R., Spoorthi, M.L. and Hemalatha, J.G., 2021, June. A Comparative Study Of ILST and ANN Algorithm for Control of DSTATCOM. In 2021 International Conference on Design Innovations for 3Cs Compute Communicate Control (ICDI3C) (pp. 45-50). IEEE.

[11] Chenchireddy, K., Kumar, V., Sreejyothi, K.R. and Tejaswi, P., 2021, December. A Review on D-STATCOM Control Techniques for Power Quality Improvement in Distribution. In 2021 5th International Conference on Electronics, Communication and Aerospace Technology (ICECA) (pp. 201-208). IEEE.
[12] Amoozegar, D., 2016. DSTATCOM modelling for voltage stability with fuzzy logic PI current controller. International Journal of Electrical Power & Energy Systems, 76, pp.129-135.
[13] Mangaraj, M. and Panda, A.K., 2017. Performance analysis of DSTATCOM employing various control algorithms. IET Generation, Transmission & Distribution, 11(10), pp.2643-2653.
[14] Swetha, K. and Sivachidambaranathan, V., 2019. A review on different control techniques using DSTATCOM for distribution system studies. Int J Pow Elec & Dri Syst, 10(2), pp.813-821.
[15] Woo, J.H., Wu, L., Lee, S.M., Park, J.B. and Roh, J.H., 2021. D-STATCOM dq axis current reference control applying DDPG algorithm in the distribution system. IEEE Access, 9, pp.145840-145851.
[16] Das, E., Banerji, A. and Biswas, S.K., 2017, December. State of art control techniques for DSTATCOM. In 2017 IEEE Calcutta Conference (CALCON) (pp. 268-273). IEEE.
[17] Negi, P., Pal, Y. and Leena, G., 2017. A Review of Various Topologies and Control Schemes of DSTATCOM Implemented on Distribution Systems. Majlesi Journal of Electrical Engineering, 11(1), p.25.
[18] Hao, P., Zanji, W. and Jianye, C., 2007. Study on the control of shunt active DC filter for HVDC systems. IEEE transactions on power delivery, 23(1), pp.396-401.

